Use of nonelectrolytes reveals the channel size and oligomeric constitution of the *Borrelia burgdorferi* P66 porin.

Marcus Thein[1,*], Iván Bárcena-Uribarri[1,*], Elke Maier[1], Mari Bonde[2], Ignas Bunikis[2], Sven Bergström[2] and Roland Benz[1]

[1]Department of Biotechnology, Biocenter, Universität Würzburg, Würzburg, Germany;
[2]Department of Molecular Biology, Umeå University, Umeå, Sweden;

*Both authors contributed equally to this work;

Keywords: nutrient uptake, outer membrane transport, Lyme disease, porin radius determination, black lipid bilayer, Blue Native PAGE.

ABSTRACT

The outer membrane protein P66 of the Lyme disease spirochete *Borrelia burgdorferi* is capable of pore formation with an atypical high single-channel conductance of 11 nS in 1 M KCl. We studied in a non-theoretical manner the diameter of the P66 channel by analyzing its single-channel conductance in black lipid bilayers in the presence of different nonelectrolytes with known hydrodynamic radii. Furthermore, we calculated the filling of the channel with these nonelectrolytes and the results revealed that nonelectrolytes with hydrodynamic radii of 0.34 nm or smaller pass through the pore, whereas neutral molecules with greater radii only partially filled the channel or were not able to enter it at all. Thus, the diameter of the P66 entrance was determined to be ≤ 1.9 nm with a constriction site diameter of about 0.7 nm. Furthermore, the P66-induced membrane conductance could be blocked by 80-90% after addition of the nonelectrolytes PEG 400, PEG 600 and maltohexaose in the low millimolar range. Interestingly, the analysis of the power density spectra of P66 after blockage with nonelectrolytes revealed no chemical interaction responsible for channel block. The blockage of one P66 single-channel conductance unit of 11 nS occurred by seven subconducting states, thus indicating a heptameric organization of the P66 oligomer. This organization of P66 as a heptamer was confirmed by Blue Native PAGE and immunoblot analysis, which demonstrated that P66 forms a complex with a mass of approximately 460 kDa.

INTRODUCTION

P66 is a protein present in the outer membranes of Lyme disease and relapsing fever spirochetes (1). The P66 found in the Lyme disease species *Borrelia burgdorferi* is well described and exhibits dual function. Firstly, it has been shown to act as an adhesin which can bind to β3-integrin (2-4); and secondly, it acts as a porin in the outer membrane (1, 5, 6). In addition, P66 contains surface-exposed domains (7, 8) and exhibits a certain immunogenic potential (9). Considering these properties, P66 appears to be an outer membrane protein with promising potential in terms of developing a vaccine candidate against Lyme disease.

The electrophysiological properties of the *B. burgdorferi* P66 channel have been studied previously in detail. P66 is able to form pores in planar lipid bilayers with a enormously high single-channel conductance of 11 nS in 1 M KCl (1). The channels are nonselective for small anions or cations and exhibit voltage-dependent closure (1, 5). Whilst certain other spirochetes porins such as those from *Spirocheta aurantia* and *Treponema denticola* also exhibit extremely high single-channel conductance (10), this is atypical and rare for Gram-negative bacterial porins. To date, besides selectivity and estimated pore diameters, very little is understood about the apparent pore size and the structure of these outer membrane channels.

The channel diameter of P66 has been calculated to be approximately 2.6 nm (5), which is rather large compared to other pore-forming outer membrane proteins (11). This calculation of the P66 channel diameter was based on the assumption that the conductance of the channel is equal to the conductivity of a simple cylinder of aqueous salt solution. The length of the cylinder was taken to be equal to the thickness of the membrane. This method should be considered as zero-order approximation, because it does not take into account important parameters such as the form of the channel and repulsion of the ions from the hydrophobic zone of the lipid membrane. Therefore, the calculated value of the P66 diameter appears to be somewhat preliminary and its apparent size and structure remain unclear.

To answer this question, the conductance of the P66 channel reconstituted in planar lipid membranes using nonelectrolytes (NEs) was studied as a function of its spherical size (12). These polymers were used successfully to determine the effective diameters of a number of polyene- and protein-induced channels (12-22). Besides, this method avoids the potentially strong coulombic interactions that occur when using ionic probes and ion channels containing fixed charges. This study therefore attempted to measure the channel diameter of P66 and to reveal partially its molecular organization in the outer membrane of *Borrelia* species.`

MATERIAL AND METHODS

Isolation and purification of P66 protein. Pure P66 was obtained by anion exchange chromatography of outer membrane fractions of *B. burgdorferi* B31 (23) as has been described previously (1, 6).

Planar lipid bilayer assays. The methods used for black lipid bilayer experiments have been described previously (24). The instrumentation consisted of a Teflon chamber with two compartments containing a 1M KCl salt solution. The two compartments were separated by a thin wall and connected by a 0.4 mm^2 small circular hole. The membranes were formed spreading a 1% (w/v) solution of diphytanoyl phosphatidylcholine (PC) (Avanti Polar Lipids, Alabaster, AL) in *n*-decane over the hole. The porin-containing protein fractions were 1:1 or 1:100 diluted in 1% Genapol (Roth) and added to the aqueous phase after the membrane had turned black. The membrane current was measured with a pair of Ag/AgCl electrodes with salt bridges switched in series with a voltage source and a highly sensitive current amplifier (Keithley 427). The temperature was kept at 20°C throughout.

In the experiments carried out to determine the channel diameter of P66, the electrolyte solution also contained right from the start 20% (w/v) of an appropriate NE as described previously (19-21). The following NEs were used: ethylene glycol (Sigma), glycerol (Sigma), arabinose (Sigma),

sorbitol (Sigma), maltose (Sigma), polyethylene glycol (PEG) 300, PEG 400 (Fluka), PEG 600 (Fluka), PEG 900 (Fluka), PEG 1000 (Fluka), PEG 2000 (Fluka), PEG 3000 (Fluka) and PEG 6000 (Fluka). Polyethylene glycols were the molecules of choice in our studies because in aqueous solutions they have a spherical shape (25, 26). By statistical analysis of at least 100 reconstituted P66 channels into lipid membranes the single-channel conductance in the presence of the different NEs was evaluated.

The conductivity of each buffer was measured with a multi-range conductivity meter (Knick laboratory conductivity meter 702) using a 4-electrode sensor (Knick ZU 6985 conductivity sensor).

Blocking of P66 conductance by NEs was investigated in the same way as the binding of maltooligosaccharides to carbohydrate-specific porins (27, 28). The measurements were performed with one single-channel of 11nS or multi-channel membranes under stationary conditions reached about 90 minutes after adding the protein. At that point NEs were added in defined concentrations to both sides of the membrane while stirring constantly to allow equilibration. Blockage of the channel conductance by NEs could be detected by an impaired ion flux through the channel reducing the conductance.

The noise analysis performed has been described previously (29-32). The membrane current was measured with a pair of silver/silver chloride electrodes switched in series with a battery-operated voltage source and a current amplifier (Keithley 427 with a four pole filter). Feedback resistors of the current amplifier were between 0.01 and 10 GΩ. The amplified signal was monitored with a strip chart recorder (Rikadenki) and fed simultaneously through a low-pass filter (4 Pole Butterworth Low-pass Filter) into an AD-converting card of an IBM-compatible PC. The digitalized data were analyzed with a home-made fast Fourier-transformation program. The spectra were composed of 400 points and they were averaged 128 or 256 times. The obtained power density spectra were further analyzed using commercial graphics programs.

Evaluation of the channel diameter with nonelectrolytes. The method of determining the pore size of P66 by using NEs is based on previously published work (19-21, 33). This type of evaluation can be used to determine the size of the channel and possible constrictions by analyzing the relationship between the single channel conductance in the presence of NEs and the NEs hydrodynamic radii.

The determination of the channel radius is based in two principles. First, a salt solution with 20% of a NE will show a reduced conductivity to 40 -70%. And second, the decrease in conductivity will only affect the conductance of the channel when the NE used is small enough to penetrate the pore. Otherwise, the solution inside the channel will be free of NEs and the conductance of the channel will be equal to the one observed when using only the salt solution. That way, the channel diameter can be considered equal to the smallest NE that does not enter the channel and therefore does not reduce its conductance.

To determine a possible constriction inside the channel the channel filling (F) was used in this study in a similar manner as published elsewhere (20). Therefore, it is assumed that an ion channel can be treated as an equivalent ohmic resistor with resistance (R). This assumption can be extended to all channels with a linear current-voltage relationship. This condition is met for P66 because the current-voltage relationship of the channel is linear as described in previous studies (1). R can be seen as composed of two parts. One part corresponds to the portion of the channel length filled with the NE (F) and one part corresponds to the portion without NE (1-F). Thus, R can be written as:

$$R = [F/(AX_i) + (1-F)/(AX_o)] \quad (1)$$

with $A = \pi r^2/l$, l is the channel length and r its radius, and X_o and X_i are the conductivities of the solution without and with NE, respectively. In assuming that AX_o is equal to the ion channel conductance in a solution without NE (G_o), it can be shown that the filling (F) is given by:

$$F = [(G_o-G_i)/ G_i]/[(X_o -X_i)/ X_i] \quad (2)$$

where G_o is the single-channel conductance in a solution without NE (1 M KCl), G_i is the single-

channel conductance in the presence of a solution containing 20% (w/v) of an NE with access to the channel interior, X_0 is the conductivity of the solution without NE (1 M KCl), and X_i is the conductivity of the solution containing 20% (w/v) of a given NE.

Assuming that the filling of the channel by two of the smallest NE (in our study ethylene glycol and glycerol) is close to the maximum possible level, the filling can be calculated in terms of percentage (*F%*):

$$F\% = 2F_i/(F_1+F_2)*100\% \quad (3)$$

where F_i is the filling in the presence of a given NE and F_1 and F_2 represent filling in the presence of ethylene glycol and glycerol in the bathing solution, respectively.

Analyzing the filling of a channel three events are possible. If the NEs are smaller than the narrowest part of the channel, it will be filled completely (F%=100%). On the other hand, if the NEs are bigger than the entrance, there will be no NE inside the channel (F%=0%). Intermediate-sized NEs will fill the channel to an extent inversely related to theirs sizes (F% between 0 and 100%). These NEs don't fill the channel completely because its size is too big getting stopped somewhere along the channel interior.

According to this method, the radius of the constriction zone should be equal to the radius of the smallest NE that does not pass freely through the channel.

Blue Native PAGE and Western blotting analyses. Blue native polyacrylamide gel electrophoresis (Blue native PAGE) was performed according to previously published protocols (34). 50 µl (approximately 50 ng) of purified P66 was separated in a 4-13% Blue native PAGE. The NativeMark Unstained (Invitrogen) and the HMW Native Marker (Amersham Biosciences) were used as molecular mass standards. For visualization of the proteins, the Blue native gels were silver stained according to a previously published protocol (35).

For Western blotting, a tank blot system (Amersham Biosciences) was used as described elsewhere (36). Bound antibodies were detected using peroxidase-conjugated anti-rabbit antibodies (DAKO A/S) and enhanced chemiluminescence reagents according to the manufacturer's instructions (Amersham Biosciences). The production and use of polyclonal rabbit serum against *B. burgdorferi* P66 has been described in previous studies (8, 37).

RESULTS

Effects of nonelectrolytes on P66 single-channel conductance.

Large nonpermeant NEs with hydrodynamic radii between 0.94 and 2.50 nm (PEG 1000, PEG 3000 and PEG 6000) did not enter the P66 channel and showed no effect on its conductance. However, in the presence of small NEs with hydrodynamic radii up to 0.60 nm, such as ethylene glycol, glycerol, arabinose, sorbitol, maltose and PEG 300, the P66 single-channel conductance decreased proportional to that of the bulk solution conductivity (Table 1). Histograms of four representative NEs measurements together with the recordings of single-channel traces are illustrated in figure 1.

Surprisingly, the presence of PEG 400 and PEG 600 (hydrodynamic radii of 0.70 and 0.80 nm, respectively) in the bathing solution resulted in an exceptional low single-channel conductance of 0.9 nS that was not proportional to the bulk aqueous conductivity. This effect appeared to be due to an interaction between the polymer and the channel interior resulting in a blockage of the conductance and was further investigated in a separate set of experiments (see below).

P66 pore size estimation.

The entrance radius of P66 is equal to 0.9 nm considering the radius of a water-filled channel equal to the minimal size of a NE that does not decrease its *G*.**.** In order to characterize the pore size, the decrease of P66 conductance was evaluated as a function of the molecular mass and hydrodynamic radii of different NEs (Table 1). The ratios of the single-channel conductance in the presence of NEs to that in the absence of NEs are shown in figure 2. The obtained results suggested that NEs with a mean molecular mass (*Mr*) of ≤ 600 g/mol and a hydrodynamic radius (*r*) ≤ 0.8 nm enter the pore whereas NEs with a

Mr ≥ 1000 g/mol and *r* ≥ 0.94 nm cannot enter the P66 channel.

It is pertinent to introduce the channel filling in order to correctly determine the size of the P66 channel (20). The channel filling *F* and the channel filling in terms of percentage *F%* were calculated according to equations 2 and 3 and are listed in table 2. The results of the dependence of *F%* on the hydrodynamic radii of the NEs are shown in figure 3. If the radius of the NEs did not exceed 0.34 nm, *F%* was always close to 100%, as it was the case for ethylene glycol (*r* = 0.26 nm), glycerol (*r* = 0.31 nm) and arabinose (*r* = 0.34 nm). Further increase of *r* caused a decrease in the filling parameter. In this way sorbitol (*r* = 0.39 nm) is able to fill the channel by only 65.8% and PEG 300 (*r* = 0.60 nm) by 42.6%.

Channel filling by PEG 400 and PEG 600 was not included in this diagram because *F%* of these NEs exceeded 100% by several orders of magnitude indicating a special interaction between channel interior and NE that was not reported to date in similar studies. Maltose (*r* = 0.50 nm) with a larger radius than sorbitol (*r* = 0.39 nm) filled approximately 100% of the channel, showing also some kind of interaction with the channel interior. Measurements with PEG 200 which has the same hydrodynamic radius as maltose showed a *F%* of 64.1%, which is coherent with the inversely decrease of the F% as the hydrodynamic radius increases.

As proposed from the plot in figure 3, the radius of the P66 entrance can be estimated from the intersection point between the dependent part of *F%* on the NEs hydrodynamic radii with the lower plateau. The radius of a possible constriction zone should be equal to the radius of the smallest NE that do not pass freely through the channel and do not fill it completely *(F%* lower than 100%). In this way, the estimated P66 entrance radius is equal to 0.9±0.1 nm with an inner constriction zone of 0.39±0.1 nm. The error of the pore radius estimation may be derived from the standard deviation of NEs radii, usually around 0.1 - 0.2 nm (21).

Interactions of nonelectrolytes with the P66 channel.

The results of P66 single-channel measurements demonstrated that the addition of PEG 400 and PEG 600 caused a decrease of the channel conductance to a higher extent (i.e., ~92% for both PEGs) than they decreased the bulk conductivity (i.e., by 58% and 51%, respectively). To investigate if this finding was caused by a specific interaction of these PEGs with the P66 channels, we performed multi-channel titration experiments as described previously (27, 28). PEG 400 and PEG 600 were added to the bathing solution where multiple P66 channels were reconstituted in artificial lipid membranes. Other NEs such as fructose, glucose, maltose, sucrose, maltohexaose and related carbohydrates were also tested.

Only the addition of small amounts of PEG 400, PEG 600 and maltohexaose to the bathing solution where P66 was reconstituted caused a substantial, dose-dependent blockage of the conductance. Figure 4 shows experiments with PEG 600 (Fig. 4A) and maltohexaose (Fig. 4B). The P66-induced conductance could be blocked by 80% after addition of 4.5 mM PEG 400 or PEG 600 and by approx. 90% after the addition of 45 mM maltohexaose. The kinetics of the decrease of P66-mediated conductance after addition of PEG 400 or PEG 600 was remarkably slow, lasting about 10-30 min, compared to the effect after addition of maltohexaose, which was somewhat faster (see Figure 4). Titrations with smaller NE molecules such as the monosaccharides fructose and glucose or the disaccharides maltose and sucrose did not lead to any blockage of the P66-induced conductance (data not shown).

Effect of PEG400 and PEG600 on a P66 single-channel.

Additional measurements were performed to study PEG 400-induced block of the P66 channel on the single-channel level. P66 was added in very small concentration to both sides of a black PC membrane. After reconstitution of one single 11 nS P66 unit into the membrane, PEG 400 was added at both sides of the membrane to a 90 mM final concentration. The addition of PEG 400 resulted in a substantial blockage of the ionic current through the channel. The recording of such a measurement is shown in figure 5 and revealed a PEG-induced, stepwise closing of P66 in seven substates. The conductance all substates was fairly homogenous and was on average about 1.5 nS. Only sporadic fluctuations of the substates were observed indicating that they were not

irreversibly closed. However, they opened with the same conductance of 1.5 nS in 1 M KCl.

Measurements of the current noise through the open and the nonelectrolyte-induced closed state of the P66 channel.

The data of Fig. 4 indicated that the decrease in conductance after addition of PEG 600 is remarkably slow and lasting 10-30 min, although continuous stirring result in much faster equilibration of the aqueous phase. To gather some information on the blocking process and its binding kinetics, we studied the current noise of the blocked P66 channels. Parallel to the titration measurements, the frequency-dependence of the spectral density of the current noise was analyzed using fast Fourier transformation. Fig. 6 illustrates an example of a measurement with PEG 600. Before addition of NEs, a reference spectrum was taken to obtain the current noise of the open P66 channel, which exhibited $1/f$ -noise in the frequency range between 10 Hz and 100 Hz (Fig. 6, trace 1). The increase of the spectral density at frequencies above about 300 Hz was caused by intrinsic noise of the preamplifier that produces a frequency-dependent current noise through the membrane capacity C_m. The reference spectrum was subtracted from each spectrum taken after the successive addition of NEs in increasing concentrations. Figure 6, trace 2 shows a spectrum taken after addition of PEG 600 (9.6 mM; the reference spectrum of trace 1 was subtracted). The current noise spectrum of P66 after addition of PEG 600 could be fitted to a $1/f$-function and is shifted to higher spectral density as compared to the reference spectrum (sees Fig. 6, trace 2). In further measurements, the concentration of PEG 600 was increased in defined steps. At other concentrations of PEG 600 (18.7 mM and 30.0 mM) the power density spectrum corresponded to that of traces 3 and 4, respectively, in figure 6, which also could be fitted to a $1/f$-function. This type of noise is expected for diffusion processes through open channels (32, 38). The spectral density of current noise through P66 channels could also be fitted to $1/f$ functions after addition of PEG 400 and maltohexaose (data not shown).

Blue native PAGE analysis of the P66 constitution.

The use of SDS-PAGE to analyze P66 did not indicate the formation of any oligomers. SDS is a detergent with denaturing properties for some protein complexes and therefore BN-Page was used. When analyzing the prepurified P66 in this native gels a band of approximately 460 KDa appeared (Figure 7, left panel). An immunoblot of the Blue native PAGE was performed using polyserum against *B. burgdorferi* P66 (8, 37). The same band of approximately 460 kDa displayed a strong positive immunoblot signal (Figure 7, right panel).

DISCUSSION

P66 pore diameter is smaller than predicted.

Estimations based on the previously reported single-channel conductance of 9.6 nS predicted that the P66 channel should have a diameter of 2.6 nm (5). This rough estimate does not take into account several effects that may influence ion conductance through a channel such as the action of image force, a more hydrophobic interior or that channel friction hinders ion movement (39, 40). Thus, to get an idea of the effective pore diameter of a channel with such an extremely high single-channel conductance as P66, pore sizing by use of NEs seemed to be a suitable method as has been demonstrated previously (Krasilnikov, 2002).

The estimation of the P66 pore size based on our single-channel measurements with different NEs indicated an entrance pore diameter of approximately 1.9 nm with a 0.8 nm inner constriction.

The estimation of the pore diameter by the use of NEs is more precise but still encounters some difficulties and assumptions. For example, the smearing of the molecular mass of the PEGs over a considerable range, which could influence the channel filling and thus the estimated radius. However, this effect is accounted and may influence only the standard deviation of the estimated radius.

Whether PEG 400 and PEG 600 molecules retain their spherical structure inside the P66 channel could be questioned. However, the consistency of the pore sizing with NEs and the comparison with results of electron microscopical investigation of ion channel structures suggests that this point does not represent a major problem (21).

A 1,9nm entrance diameter is within the range of other several gram-negative bacterial porins and other membrane channels, that were characterized by the use of NEs, such as *Bacillus anthracis* $(PA_{63})_7$ ($d \approx 2$ nm) (41), *Staphylococcus aureus* α-toxin ($d \approx 1.35$ nm) (21) and the colicin Ia ion channel ($d \approx 1$ nm) (20). These three channels exhibit single-channel conductances of ~180 pS in 1 M KCl (42), 775 pS in 1 M KCl (43) and ~90 pS in 1.77 M KCl (20), respectively. P66 has an apparent channel diameter close to the one of *Bacillus anthracis* $(PA_{63})_7$, but its single-channel conductance is about 60-fold higher than the $(PA_{63})_7$ one.

The high discrepancy between the channel conductance and channel radius cannot only be explained by special effects in the channel lumen. The molecular organization of the P66 complex seems to play a major role as discussed below in more detail.

The effects of PEG 400 and PEG 600 on the P66 single-channel conductance are caused by a special interaction with the channel interior.

Membrane experiments in the presence of 20 % PEG 400 or PEG 600 resulted in drastically reduced single-channel conductance. The decrease of ion flux through the channel was significantly greater than the measured decrease of the bulk conductivity after addition of NEs and was also observed during multi-channel measurements which revealed that the P66 conductance could be blocked by 80-90% after the addition of PEG 400, PEG 600 and maltohexaose. Interestingly, kinetics of conductance decrease after addition of these compounds was very slow, an observation that differs from substrate-binding porins (31, 44, 45). This finding enforced the assumption that specific interactions of PEG 400, PEG 600 and maltohexaose with the channel interior result in the block of the ion flux through the pore. Measurements of the current noise through open and NE-induced closed states of P66 channels should reveal the possible binding kinetics of this interaction during the blocking effect. Current noise measurements and the analyses of the resulting power density spectra obtained by Fourier-transformation allow studying the binding kinetics of substrate-specific porins (29, 30, 44, 45). In these cases the noise is of Lorentzian type. Analysis of this Lorentzian type of noise yields the rate constants and thus a determination of the binding kinetics. Open channel noise of general diffusion porins and porins with a binding site for a specific substrate shows in contrast to this a $1/f$-noise (31, 32, 38).

Open P66 channels exhibited $1/f$-noise before addition of NEs, similar as the noise of other open porin channels (32). But in contrast to well-studied substrate-specific porins, P66 channels exhibited also $1/f$-noise after blockage of the P66-induced conductance by addition of NEs. $1/f$-noise is known to describe diffusion processes through open bacterial channels (32, 38), meaning that there was no chemical reaction, e.g. substrate binding, detectable during the interaction of NEs with the P66 channel. This phenomenon is exceptional for substrate-specific porins and detailed kinetics during the blockage of the P66-induced conductance remain unclear.

Anyway, these studies were focusing more on the blocking effect of P66-induced membrane conductance than on the determination of permeation kinetics and the possible spectrum of the P66 substrate-specificity. Thus, further investigations have to be done to understand the binding and permeation kinetics of NEs in more detail. In particular, the interacting domains of both the NEs and the P66 lumen are not known and can only be derived definitely from deeper structural insights such as X-ray analyses of P66 crystals.

The discrepancy between single-channel conductance and effective diameter suggested that the channel-forming domain of P66 is composed of several subunits.

Several experimental observations suggest that the P66 channel is not formed by a P66 monomer alone. First of all, the size of the channel as derived from measurement with NEs does not agree with its extremely high single-channel conductance of about 11 nS in 1 M KCl (1). Furthermore, the stepwise block of the P66 channel with certain NEs occurred in seven substates with a conductance of about 1.5 nS in 1 M KCl. All these results suggested that the P66 channel may be formed by a bundle of pores.

To support this view, purified P66 was investigated by Blue native PAGE, a method that allows the determination of native protein masses and oligomeric states of protein complexes (34). A

460 kDa band agree with the oligomeric theory as a P66 heptamer would have a molecular mass of 462 kDa. Furthermore, the six or seven substates with a conductance of about 1.5 nS could match the 11 nS conductance of the oligomer.

Taken together, the results presented here suggested that the individual P66 molecules are forming a high molecular mass protein complex, possibly a heptamer. The individual channels in the oligomer act like molecular sieves with a molecular mass cut-off of 182 g/mol and an exclusion size smaller than 1 nm. If that is the case, P66 could be the first known example of a porin constituted by a bundle of seven independent channels in a protein complex. Such a structure was to date only observed in *Borrelia*, but not in any other bacterium or any other living organisms.

ACKNOWLEDGEMENTS

The authors thank Martin Mau for his help with lipid bilayer measurements. The Alfonso Martín Escudero Foundation is thanked for financial support to Iván Bárcena-Uribarri during the research process. This work was supported by the joint project between Stint (Sweden) and DAAD (Germany) to SB and RB, by the Fonds der Chemischen Industrie (to RB) and the Swedish Medical Research Council (to SB).

REFERENCES

1. Barcena-Uribarri, I., M.Thein, A. Sacher, I. Bunikis, S. Bergström, and R. Benz. 2009. P66 porins are present in both Lyme disease and relapsing fever spirochetes: a comparison of the biophysical properties of P66 porins in six *Borrelia* species. Manuscript.
2. Coburn, J., W. Chege, L. Magoun, S. C. Bodary, and J. M. Leong. 1999. Characterization of a candidate *Borrelia burgdorferi* beta3-chain integrin ligand identified using a phage display library. Mol Microbiol 34:926-940.
3. Defoe, G., and J. Coburn. 2001. Delineation of *Borrelia burgdorferi* p66 sequences required for integrin alpha(IIb)beta(3) recognition. Infect Immun 69:3455-3459.
4. Coburn, J., and C. Cugini. 2003. Targeted mutation of the outer membrane protein P66 disrupts attachment of the Lyme disease agent, *Borrelia burgdorferi*, to integrin alphavbeta3. Proc Natl Acad Sci U S A 100:7301-7306.
5. Skare, J. T., T. A. Mirzabekov, E. S. Shang, D. R. Blanco, H. Erdjument-Bromage, J. Bunikis, S. Bergström, P. Tempst, B. L. Kagan, J. N. Miller, and M. A. Lovett. 1997. The Oms66 (p66) protein is a *Borrelia burgdorferi* porin. Infect Immun 65:3654-3661.
6. Pinne, M., M. Thein, K. Denker, R. Benz, J. Coburn, and S. Bergström. 2007. Elimination of channel-forming activity by insertional inactivation of the p66 gene in *Borrelia burgdorferi*. FEMS Microbiol Lett 266:241-249.
7. Bunikis, J., L. Noppa, Y. Ostberg, A. G. Barbour, and S. Bergstrom. 1996. Surface exposure and species specificity of an immunoreactive domain of a 66-kilodalton outer membrane protein (P66) of the *Borrelia* spp. that cause Lyme disease. Infect Immun 64:5111-5116.
8. Bunikis, J., L. Noppa, and S. Bergström. 1995. Molecular analysis of a 66-kDa protein associated with the outer membrane of Lyme disease *Borrelia*. FEMS Microbiol Lett 131:139-145.
9. Barbour, A. G., A. Jasinskas, M. A. Kayala, D. H. Davies, A. C. Steere, P. Baldi, and P. L. Felgner. 2008. A genome-wide proteome array reveals a limited set of immunogens in natural infections of humans and white-footed mice with *Borrelia burgdorferi*. Infect Immun.
10. Egli, C., W. K. Leung, K. H. Muller, R. E. Hancock, and B. C. McBride. 1993. Pore-forming properties of the major 53-kilodalton surface antigen from the outer sheath of *Treponema denticola*. Infect Immun 61:1694-1699.
11. Benz, R. 1985. Porin from bacterial and mitochondrial outer membranes. CRC Crit Rev Biochem 19:145-190.
12. Krasilnikov, O. V. 2002. Sizing channels with neutral polymers. In Structure and Dynamics of Confined Polymers. K. Press, editor. Kasianowicz, J. J., Kellermayer M. S. Z., Deamer, D. W., Dordrecht, Netherlands. 97-115.
13. Rostovtseva, T. K., E. M. Nestorovich, and S. M. Bezrukov. 2002. Partitioning of differently sized poly(ethylene glycol)s into OmpF porin. Biophys J 82:160-169.
14. Berestovsky, G. N., V. I. Ternovsky, and A. A. Kataev. 2001. Through pore diameter in the cell wall of *Chara corallina*. J Exp Bot 52:1173-1177.
15. Kaulin, Y. A., L. V. Schagina, S. M. Bezrukov, V. V. Malev, A. M. Feigin, J. Y. Takemoto, J. H. Teeter, and J. G. Brand. 1998. Cluster organization of ion channels formed by the antibiotic syringomycin E in bilayer lipid membranes. Biophys J 74:2918-2925.
16. Ternovsky, V. I., Y. Okada, and R. Z. Sabirov. 2004. Sizing the pore of the volume-sensitive anion channel by differential polymer partitioning. FEBS Lett 576:433-436.
17. Vodyanoy, I., and S. M. Bezrukov. 1992. Sizing of an ion pore by access resistance measurements. Biophys J 62:10-11.
18. Holz, R., and A. Finkelstein. 1970. The water and nonelectrolyte permeability induced in thin lipid membranes by the polyene antibiotics nystatin and amphotericin B. J Gen Physiol 56:125-145.
19. Sabirov, R. Z., O. V. Krasilnikov, V. I. Ternovsky, and P. G. Merzliak. 1993. Relation between ionic channel conductance and conductivity of media containing different nonelectrolytes. A novel method of pore size determination. Gen Physiol Biophys 12:95-111.
20. Krasilnikov, O. V., J. B. Da Cruz, L. N. Yuldasheva, W. A. Varanda, and R. A. Nogueira. 1998. A novel approach to study the geometry of the water lumen of ion channels: colicin Ia channels in planar lipid bilayers. J Membr Biol 161:83-92.
21. Krasilnikov, O. V., R. Z. Sabirov, V. I. Ternovsky, P. G. Merzliak, and J. N. Muratkhodjaev. 1992. A simple method for the determination of the pore radius of ion channels in planar lipid bilayer membranes. FEMS Microbiol Immunol 5:93-100.
22. McKim, S., and J. F. Hinton. 1994. Evidence of xenon transport through the gramicidin channel: a 129Xe-NMR study. Biochim Biophys Acta 1193:186-198.

23. Magnarelli, L. A., J. F. Anderson, and A. G. Barbour. 1989. Enzyme-linked immunosorbent assays for Lyme disease: reactivity of subunits of *Borrelia burgdorferi*. J Infect Dis 159:43-49.
24. Benz, R., K. Janko, W. Boos, and P. Läuger. 1978. Formation of large, ion-permeable membrane channels by the matrix protein (porin) of *Escherichia coli*. Biochim Biophys Acta 511:305-319.
25. Mark, J. E., Flory, P.J. 1965. The configuration of the polyoxyethylene chain. J. Am. Chem. Soc. 87:1415-1422.
26. Rempp, P. 1957. Contribution a l'étude des solution de molecules en chain a squelette oxigène. J. Chem. Phys. 54:432-453.
27. Benz, R., A. Schmid, T. Nakae, and G. H. Vos-Scheperkeuter. 1986. Pore formation by LamB of *Escherichia coli* in lipid bilayer membranes. J Bacteriol 165:978-986.
28. Benz, R., A. Schmid, and G. H. Vos-Scheperkeuter. 1987. Mechanism of sugar transport through the sugar-specific LamB channel of *Escherichia coli* outer membrane. J Membr Biol 100:21-29.
29. Andersen, C., M. Jordy, and R. Benz. 1995. Evaluation of the rate constants of sugar transport through maltoporin (LamB) of *Escherichia coli* from the sugar-induced current noise. J Gen Physiol 105:385-401.
30. Jordy, M., C. Andersen, K. Schulein, T. Ferenci, and R. Benz. 1996. Rate constants of sugar transport through two LamB mutants of *Escherichia coli*: comparison with wild-type maltoporin and LamB of *Salmonella typhimurium*. J Mol Biol 259:666-678.
31. Denker, K., F. Orlik, B. Schiffler, and R. Benz. 2005. Site-directed mutagenesis of the greasy slide aromatic residues within the LamB (maltoporin) channel of *Escherichia coli*: effect on ion and maltopentaose transport. J Mol Biol 352:534-550.
32. Wohnsland, F., and R. Benz. 1997. 1/f-Noise of open bacterial porin channels. J Membr Biol 158:77-85.
33. Krasilnikov, O. V., L. N. Yuldasheva, R. A. Nogueira, and C. G. Rodrigues. 1995. The diameter of water pores formed by colicin Ia in planar lipid bilayers. Braz J Med Biol Res 28:693-698.
34. Wittig, I., H. P. Braun, and H. Schagger. 2006. Blue native PAGE. Nat Protoc 1:418-428.
35. Schägger, H. 2006. Tricine-SDS-PAGE. Nat Protoc 1:16-22.
36. Towbin, H., T. Staehelin, and J. Gordon. 1979. Electrophoretic transfer of proteins from polyacrylamide gels to nitrocellulose sheets: procedure and some applications. Proc Natl Acad Sci U S A 76:4350-4354.
37. Sadziene, A., P. A. Rosa, P. A. Thompson, D. M. Hogan, and A. G. Barbour. 1992. Antibody-resistant mutants of *Borrelia burgdorferi*: in vitro selection and characterization. J Exp Med 176:799-809.
38. Bezrukov, S. M., and M. Winterhalter. 2000. Examining noise sources at the single-molecule level: 1/f noise of an open maltoporin channel. Phys Rev Lett 85:202-205.
39. Markin, V. S., and Y. A. Chizmadzhev. 1974. Induced Ion Transport. Nauka, Moscow.
40. Sizonenko, V. L. 1995. [The role of image charge in ionic-electrostatic interactions of proteins and membranes]. Biofizika 40:1251-1255.
41. Nablo, B. J., K. M. Halverson, J. W. F. Robertson, T. L. Nguyen, R. G. Panchal, R. Gussio, S. Bavari, O. V. Krasilnikov, and J. J. Kasianowicz. 2008. Sizing the *Bacillus anthracis* PA63 Channel with Nonelectrolyte Poly (Ethylene Glycols). Biophysical Journal 95:1157.
42. Orlik, F., B. Schiffler, and R. Benz. 2005. Anthrax toxin protective antigen: inhibition of channel function by chloroquine and related compounds and study of binding kinetics using the current noise analysis. Biophys J 88:1715-1724.
43. Menestrina, G., M. Dalla Serra, M. Comai, M. Coraiola, G. Viero, S. Werner, D. A. Colin, H. Monteil, and G. Prevost. 2003. Ion channels and bacterial infection: the case of beta-barrel pore-forming protein toxins of *Staphylococcus aureus*. FEBS Lett 552:54-60.
44. Orlik, F., C. Andersen, and R. Benz. 2002. Site-directed mutagenesis of tyrosine 118 within the central constriction site of the LamB (maltoporin) channel of *Escherichia coli*. II. Effect on maltose and maltooligosaccharide binding kinetics. Biophys J 83:309-321.
45. Andersen, C., R. Cseh, K. Schulein, and R. Benz. 1998. Study of sugar binding to the sucrose-specific ScrY channel of enteric bacteria using current noise analysis. J Membr Biol 164:263-274.

TABLES

.

Nonelectrolyte	*Mr* (*g/mol*)	*r* (*nm*)	*G* (*nS*)	X (*mS cm*$^{-1}$)
None	-	-	11.0	110.3
Ethylene glycol	62	0.26	6.5	57.2
Glycerol	92	0.31	5.5	49.1
Arabinose	150	0.34	7.0	63.7
Sorbitol	182	0.39	7.5	57.8
Maltose	360	0.50	8.0	73.8
PEG 300	300	0.60	7.5	45.5
PEG 400	400	0.70	0.9	46.4
PEG 600	600	0.80	0.9	54.1
PEG 1000	1000	0.94	12.0	49.5
PEG 3000	3000	1.44	10.5	48.9
PEG 6000	6000	2.50	10.5	50.5

Table 1. Average single-channel conductances of P66 in the presence of different nonelectrolytes (NEs) in the bath solution.
Average single-channel conductances *G* are expressed as mean of at least 100 conductance steps into a diphytanoyl phosphatidylcholine membrane in the presence of the corresponding nonelectrolyte at a concentration of 20% (w/v) in the bathing solution 1 M KCl. *Mr* = molecular mass; *r* = hydrodynamic radius; *Mr* and *r* of the nonelectrolytes were taken from previous publications (19-21); X = conductivity of the solutions, T = 24.5°C for measurements of X.

Nonelectrolyte	*r* (*nm*)	*F*	*F%*
Ethylene glycol	0.26	0.75	96.8
Glycerol	0.31	0.80	106.7
Arabinose	0.34	0.78	100.6
Sorbitol	0.39	0.51	65.8
Maltose	0.50	0.76	98.1
PEG 300	0.60	0.33	42.6
PEG 400	0.70	nl.	nl.
PEG 600	0.80	nl.	nl.
PEG 1000	0.94	-0.07	9.0
PEG 3000	1.44	0.04	5.2
PEG 6000	2.50	0.04	5.2

Table 2. Parameters for the filling of the P66 channel with nonelectrolytes.
F and *F%* are the absolute ion channel filling and the ion channel filling in terms of percentage, respectively, in the presence of 20% (w/v) nonelectrolytes in the bathing solution 1 M KCl. *F* and *F%* were calculated according to Eq. 2 and Eq. 3, respectively. nl. means neglected: the channel filling of PEG 400 and PEG 600 was neglected and not included in this table, because the calculated values of *F* and *F%* were without meaning due to possible interactions of these compounds with the channel interior (for details see text). *r* = hydrodynamic radius of the nonelectrolyte taken from previous publications (19-21);

FIGURES

Figure 1. Distribution of the single-channel conductances of P66 in the presence of nonelectrolytes. Histograms were constructed from the evaluation of at least 100 insertional events into a diphytanoyl phosphatidylcholine membrane in the presence of 20% (w/v) maltose (A), PEG 400 (B), PEG 600 (C) and PEG 1000 (D) in the bathing solution 1 M KCl. The insets show original recordings of the single-channel current vs. time. The base lines of these recordings represent the zero current level.

Figure 2. Dependence of the single-channel conductance of P66 on the molecular mass (A) and the hydrodynamic radius (B) of the nonelectrolytes. $G_{(+NE)}/G_{(-NE)}$ is the ratio of the mean single-channel channel conductance in the presence of NEs (taken from table 1) to that in the absence of NEs (11 nS (1)). Molecular masses and hydrodynamic radii of the nonelectrolytes were taken from table 1.

Figure 3. Dependence of the channel filling *F%* on the hydrodynamic radii of nonelectrolytes. *F%* for each nonelectrolyte was calculated according to Eq. 5. Lines are best fits to the experimental points. The channel filling of PEG 400 and PEG 600 was not included in this diagram, because the calculated values of *F* and *F%* were pointless high and not utilizable due to possible interactions of these compounds with the channel interior (for details see text). The horizontal lines connect the points derived from measurements in the presence of PEG 1000, PEG 3000 and PEG 6000. The other line regression was used to describe the points for the nonelectrolytes with radii ranging from 0.26 nm to 0.6 nm. Hydrodynamic radii of the nonelectrolytes were taken from table 2.

Figure 4. Titration of the P66-induced membrane conductance with PEG 600 (A) and maltohexaose (B). The membrane was formed with diphytanoyl phosphatidylcholine/*n*-decane. The aqueous phase contained ~100 ng ml^{-1} P66, 1 M KCl and respective nonelectrolytes in the concentration as indicated; temperature = 20°C; applied voltage = 20 mV.

Figure 5. PEG 400-induced blockage of P66 on the single-channel level. Small amounts of highly diluted P66 (1:1000 in 1% Genapol) was added to both sides of a diphytanoyl phosphatidylcholine membrane. After reconstitution of one single 11 nS P66 unit, 90 mM PEG 400 was added to both sides of the membrane. The P66 conductance was blocked stepwise exhibiting subconducting steps of approximately 1.5 nS; temperature = 20°C; applied voltage = 20 mV.

Figure 6. Power density spectrum of PEG 600-induced current noise of 61 P66 channels. Trace 1 shows the control, the aqueous phase contained 1 M KCl. For traces 2, 3 and 4 the aqueous phase contained 9.6 mM, 18.7 mM and 30.0 mM PEG 600, respectively, and the power density spectrum of trace 1 was subtracted from each of those traces. PEG 400- and maltohexaose-induced current noises resulted in similar power density spectra (data not shown).

Figure 7. Blue native (BN) PAGE and Western blotting (WB) analysis of the purified P66 complex. Approximately 50 ng of purified P66 was applied on a 4-13% Blue native PAGE and silver stained (BN, left panel). Western blotting of this BN-PAGE using polyserum against *B. burgdorferi* P66 resulted in a clear signal (WB, right panel). The position of molecular mass standard in kDa is shown at the left.

Figure 1

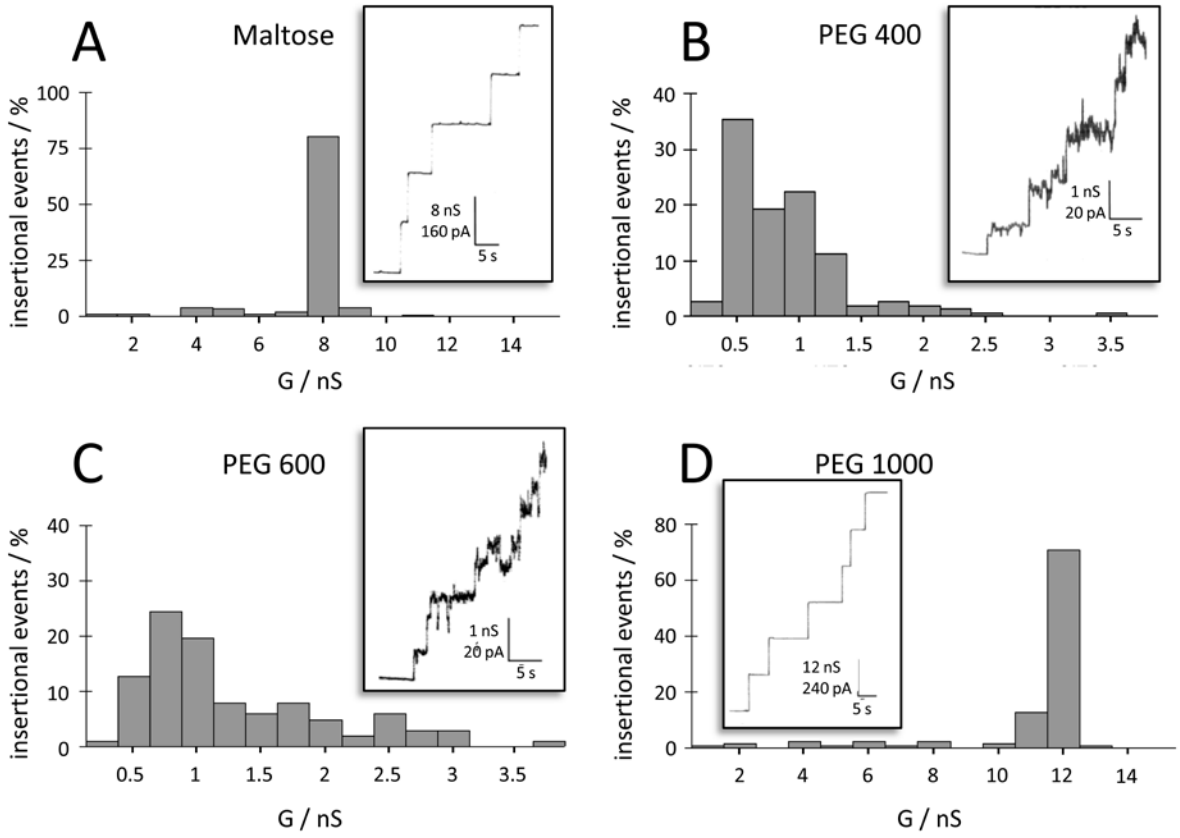
A
Maltose
insertional events / %
G / nS
8 nS
160 pA
5 s
B
PEG 400
1 nS
20 pA
5 s
C
PEG 600
1 nS
20 pA
5 s
D
PEG 1000
12 nS
240 pA
5 s

Figure 2

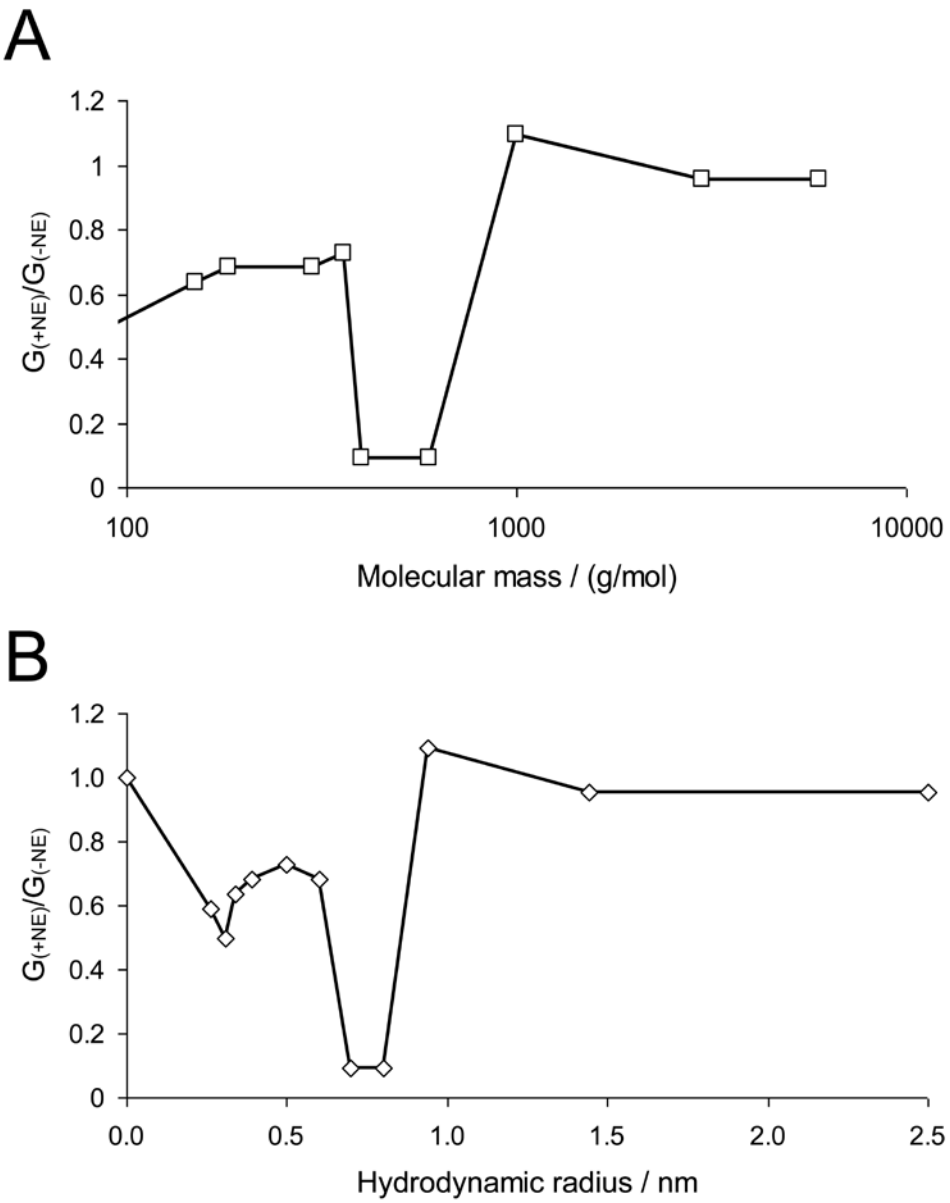
A
1.2
1
0.8
0.6
0.4
0.2
0
G(+NE)/G(-NE)
100
1000
10000
Molecular mass / (g/mol)
B
1.2
1.0
0.8
0.6
0.4
0.2
0
G(+NE)/G(-NE)
0.0
0.5
1.0
1.5
2.0
2.5
Hydrodynamic radius / nm

Figure 3

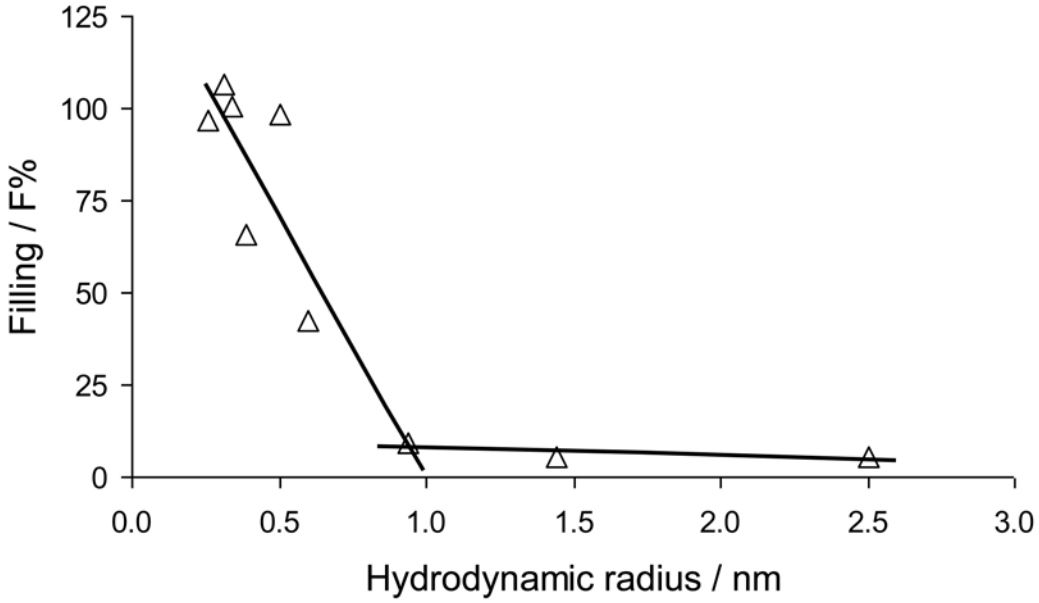
125
100
75
50
25
0
Filling / F%
0.0
0.5
1.0
1.5
2.0
2.5
3.0
Hydrodynamic radius / nm

Figure 4

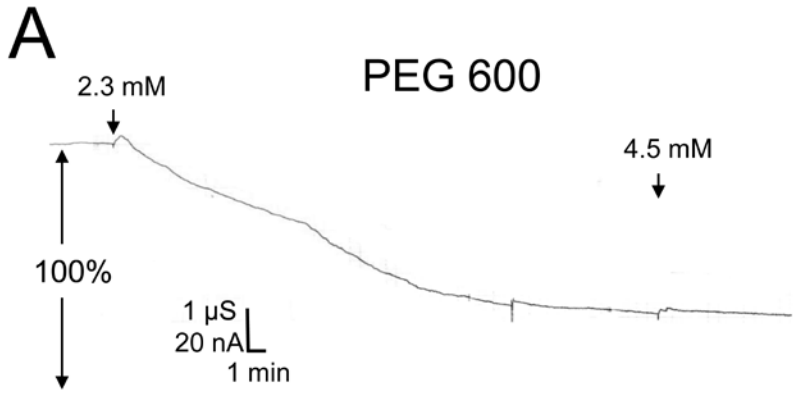
A
PEG 600
2.3 mM
4.5 mM
100%
1 µS
20 nA
1 min

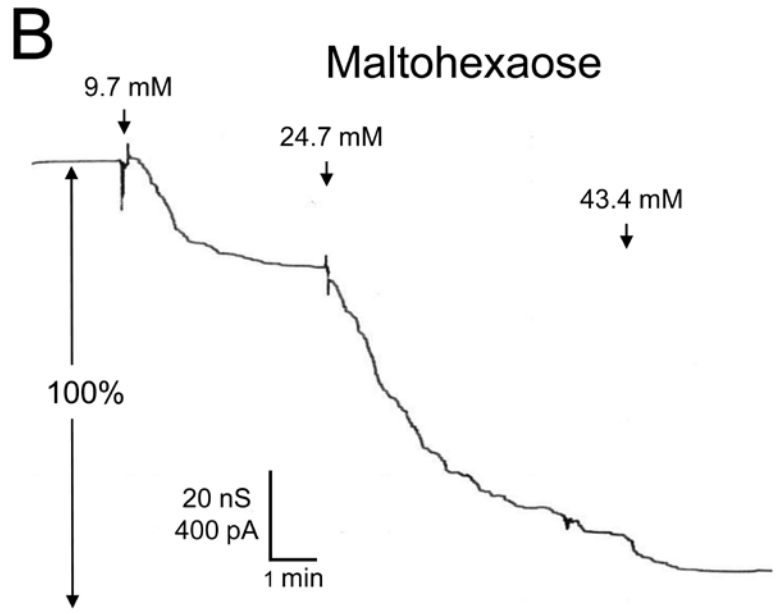
B
Maltohexaose
9.7 mM
24.7 mM
43.4 mM
100%
20 nS
400 pA
1 min

Figure 5

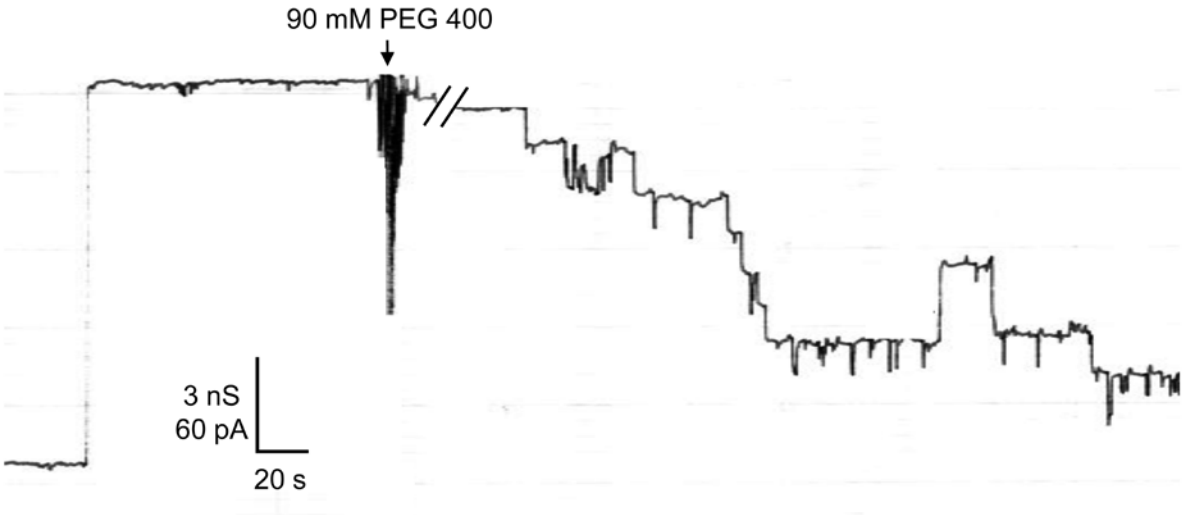

Figure 6

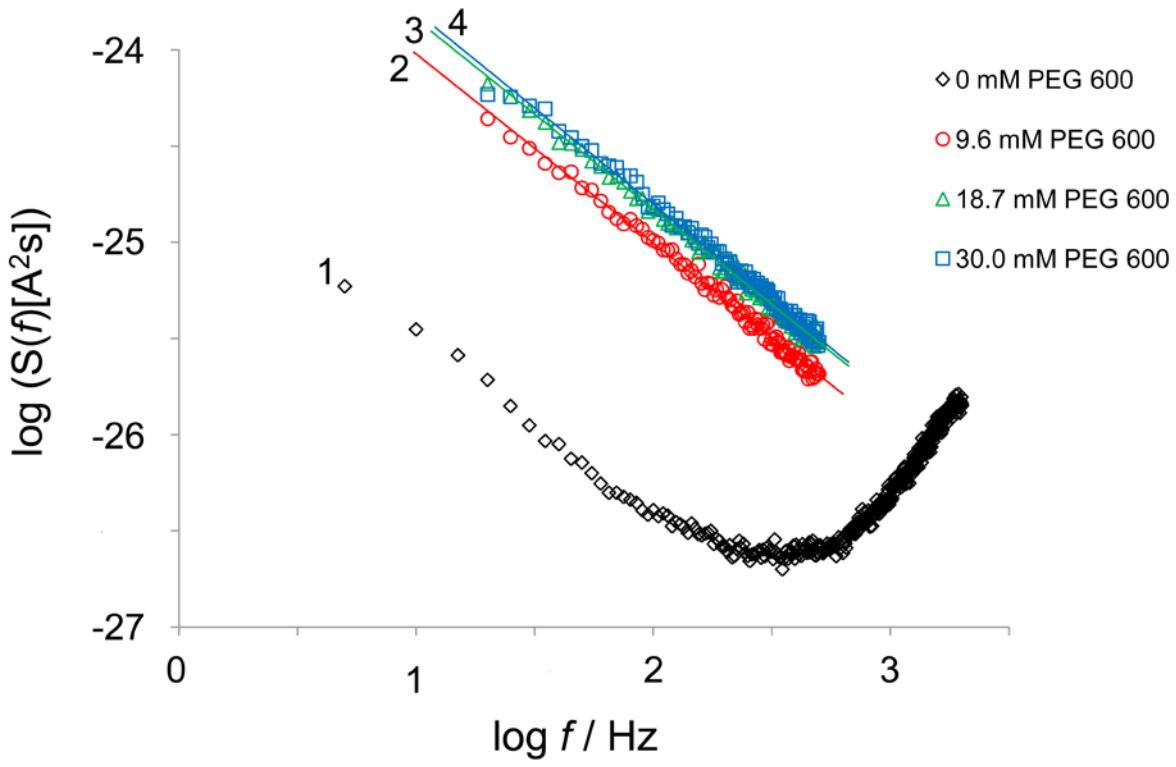
-24
-25
-26
-27
0
1
2
3
log (S(f)[A²s])
log f / Hz
1
2
3
4
0 mM PEG 600
9.6 mM PEG 600
18.7 mM PEG 600
30.0 mM PEG 600

Figure 7